Electronic Supplementary Material (ESI) for Materials Chemistry Frontiers.

Supporting Information

A responsive AIE-active fluorescent probe for visualization of acetylcholinesterase activity *in vitro* and *in vivo*

Chunbai Xiang,[a†] Musa Dirak,[b†] Yuan Luo,[a†] Yonglin Peng,[c] Lintao Cai,[a] Ping Gong,*[a] Pengfei Zhang*[a] and Safacan Kolemen*[bdef]

[a.] Guangdong Key Laboratory of Nanomedicine, CAS Key Laboratory of Health Informatics, Shenzhen Bioactive Materials Engineering Lab for Medicine, Institute of Biomedicine and Biotechnology, Shenzhen Institute of Advanced Technology, Chinese Academy of Sciences, Shenzhen 518055, China.

[b.] Department of Chemistry, Koc University, 34450 Istanbul, Turkey

[c.] Pinete (Zhongshan) Biotechnology Co., Ltd.

[d.] Surface Science and Technology Center (KUYTAM), Koc University, 34450 Istanbul, Turkey

[e.] Boron and Advanced Materials Application and Research Center, Koc University, 34450 Istanbul, Turkey

[f.] TUPRAS Energy Center (KUTEM), Koc University, 34450 Istanbul, Turkey

[†] These authors are co-first authors and contributed equally to this work.

Email: skolemen@ku.edu.tr,pf.zhang@siat.ac.cn,ping.gong@siat.ac.cn

Materials

Solvents and other common reagents were obtained from Sigma Aldrich and Energy Chemical. Phosphate buffer saline (pH=7.4) was used to prepare all aqueous solutions. Acetylcholinesterase, butyrylcholinesterase, lipase, lysozyme, trypsin, tyrosinase, lactoferrin and pepsin were purchased from Sigma-Aldrich. Carboxylesterase was purchased from Shanghai Myrell Chemical Technology Co., Ltd. Other chemicals were purchased from commercial source and used without further purification. AChE/AF350 was purchased from Shanghai Bolsen Biotechnology Co., Ltd. Mitochondrial tracker, endoplasmic reticulum tracker and lysosomal tracker were purchased from Thermo Fisher Scientific Co., Ltd.

Instruments

UV-Vis absorption spectra were recorded on a Rarian 50 Conc UV-Visible spectrophotometer. Fluorescence spectra were recorded on Edinburgh FS5 fluorescence spectrophotometer. ^{1}H NMR and ^{13}C NMR spectra were measured on a Bruker ARX 400 MHz spectrometer. High-resolution mass spectra (HRMS) were recorded on a GCT Premier CAB 048 mass spectrometer operating in MALDI-TOF mode. Cellular imaging experiments were performed with a confocal laser scanning microscope (Stellaris 5, Leica, Germany). *In vivo* imaging was performed on VISQUE® In Vivo Smart-LF imaging system.

Synthesis

Synthesis of TCFPB-AChE

TCFIS[1] (100 mg, 0.27 mmol), Compound 3[2] (132 mg, 0.40 mmol), and potassium carbonate (112 mg, 0.81 mmol) were dispersed in acetone. The reaction was refluxed overnight. The solvent was removed under reduced pressure, and the crude product was purified with the mixed solvent of PE/EA (5:1 to 2:1, v/v) to give TCFPB-AChE as a black solid (98 mg, 51.8%). ^{1}H NMR (400 MHz, DMSO-*d6*) δ 8.41 (d, J = 15.5 Hz, 1H), 7.88 (d, J = 9.1 Hz, 1H), 7.73 (d, J = 7.8 Hz, 2H), 7.31 (d, J = 8.3 Hz, 1H), 6.86 (d, J = 15.5 Hz, 1H), 6.60 – 6.52 (m, 1H), 6.36 (d, J = 2.2 Hz, 1H), 5.33 (s, 2H), 4.55 (s, 2H), 3.57 (q, J = 7.0 Hz, 4H), 3.10 (d, J = 9.0 Hz, 12H), 2.96 (s, 3H), 1.63 (s, 6H), 1.17 (t, J = 7.0 Hz, 6H). ^{13}C NMR (101 MHz, DMSO-*d6*) δ 175.75, 161.99, 153.90, 151.69, 134.11, 131.83, 124.52, 121.21, 114.41, 112.80, 98.12, 95.15, 52.61, 49.70, 45.18, 39.36, 37.19, 36.89, 26.04, 13.18. HRMS (MALDI-TOF): m/z: calcd for $C_{36}H_{43}N_6O_4$: 623.33403; found: 623.33415.

General procedures for the detection of AChE

Unless otherwise noted, all the spectral measurements were performed in 5 mM phosphate buffer (pH 7.4, containing 0.5% DMSO) according to the following procedure. AChE was dissolved in aqueous solution. The stock solution (1.0 mM) of probe TCFPB-AChE was first prepared in DMSO. 5 μL of TCFPB-AChE stock solution was added to 1 mL PBS followed by addition of different volumes of AChE solution. The mixture was incubated 4h at 37 °C, and the reaction solution was transferred to a quartz cell with an optical length of 1 cm for measurement. The excitation and emission slit were set at 5.0 nm and 5.0 nm, respectively.

Photostability

To investigate the photostability of the probe, the PL intensities of TCFPB-AChE (634 nm) in PBS solution were monitored by an Edinburgh FS5 fluorescence spectrophotometer, upon continuous irradiation with a 150 W Xe light (600 nm) of the fluorescence spectrophotometer. The photostability of TCFPB-BChE was demonstrated by plotting I/I_0 versus the irradiation time, where I is the PL intensity ratio of TCFPB-AChE after the irradiation time of t, and I_0 is the PL intensity ratio of TCFPB-AChE before light irradiation.

Determination of the detection limit of TCFPB-AChE toward addition of AChE

Based on the linear fitting in Figure 4B, the detection limit (C) is estimated as follows:

$$C = 3\sigma/K$$

Where σ is the standard deviation obtained from three individual fluorescent intensity (634 nm) of TCFPB-AChE (5 μM) without any AChE and K is the slope obtained after linear fitting the titration curves in Figure 4B.

Inhibition of Enzyme Activity

The inhibitory effect of donepezil on the enzyme activity was determined by the following procedures:
AChE (0.2 U/mL) was pre-incubated with different concentrations of donepezil in 1 mL of PBS buffer of pH 7.4 for 2h then 5 μL of TCFPB-AChE (1.0 mM in DMSO) was added. Fluorescence spectra of the solutions were recorded after incubation for another 4 h. The percent inhibition values corresponding to the presence of different concentrations of donepezil were calculated using the following equation:

$$\text{Inhibition efficiency (\%)} = 100 - [(F_i / F_o) \times 100]$$

where F_o and F_i are the fluorescence intensities obtained for AChE in the absence and presence of donepezil, respectively.

Cell Culture

The U87 cells was cultured in DMEM (containing 10% heat-inactivated FBS, 100 $mg \cdot mL^{-1}$ penicillin and 100 $mg \cdot mL^{-1}$streptomycin) at 37 °C in a humidified incubator with 5% CO_2.

Fluorescence Imaging in mice

Alzheimer's disease mice were purchased from Jiangsu ALF Biotechnology Co. Ltd (Jiangsu, China) and all animals received care incompliance with the guidelines outlined in the Guide for the Care and Use of Laboratory Animals. The procedures were approved by Shenzhen Institutes of Advanced Technology, Chinese Academy of Sciences Animal Care and Use Committee.

TCFPB-AChE(25μL, 1mM) was injected intracranially to all mice, and the images were obtained by a small animal optical *in vivo* imaging system. Brain tissue images were obtained by a small animal optical *in vivo* imaging system.

Molecular docking program

1. The crystal structure of the target protein (AChE) came from the PDB database (PDB:1B41). The protein structure was processed on the Maestro11.9 platform. The protein was processed with Schrodinger's Protein Preparation Wizard to remove crystal water, added missing hydrogen atoms, and repaired missing bonds, peptides. Finally, minimized the energy and optimized the geometric structure of the protein.[3,4]
2. The processing and optimization of molecular docking were completed by the Glide module in the Schrödinger Maestro software. Protein preparation used the Protein Preparation Wizard module. Preprocessing, optimization, and minimization of the receptor (used OPLS3e force field for constraint minimization). The compound structure was prepared according to the default settings of the LigPre module. When screening in the Glide module, imported the prepared receptor, and performed site prediction according to the structural characteristics of the protein to generate the active site position in the receptor grid. Finally, molecular docking and screening were carried out by SP method.
3. We analyzed the mode of action of the compound and the target protein to obtain the interaction between the compound and protein residues, such as hydrogen bonding, π-π interaction, hydrophobic interaction, etc., Based on the above results, we could infer whether the compound has a positive compound similar activity.

Computational Studies

We used GaussView 5.0 and Gaussian 09 software for structure visualization and simulation, respectively. The structure of the compound was optimized for the smallest energy form. The current research has realized the B3LYP function of DFT. For orbital descriptions, Pople basis set 6-31G* was used for carbon, hydrogen, nitrogen and oxygen atoms. The optimized geometries of the ground-state (S0) and excited-state (S1) minima were calculated by Gaussian 09 with TD-DFT at the level of B3LYP/6-31G*.

Figures and Tables

Table S1. The distance between the probe TCFPB-AChE and the key amino acids at the active sites of acetylcholinesterase (AChE).

Hydrogen bond distance	VAL-239	GLN-413	THR-311	Average	Binding energy: -8.42 kcal/mol
	3.3 Å	2.6 Å	3.4 Å	3.1 Å	

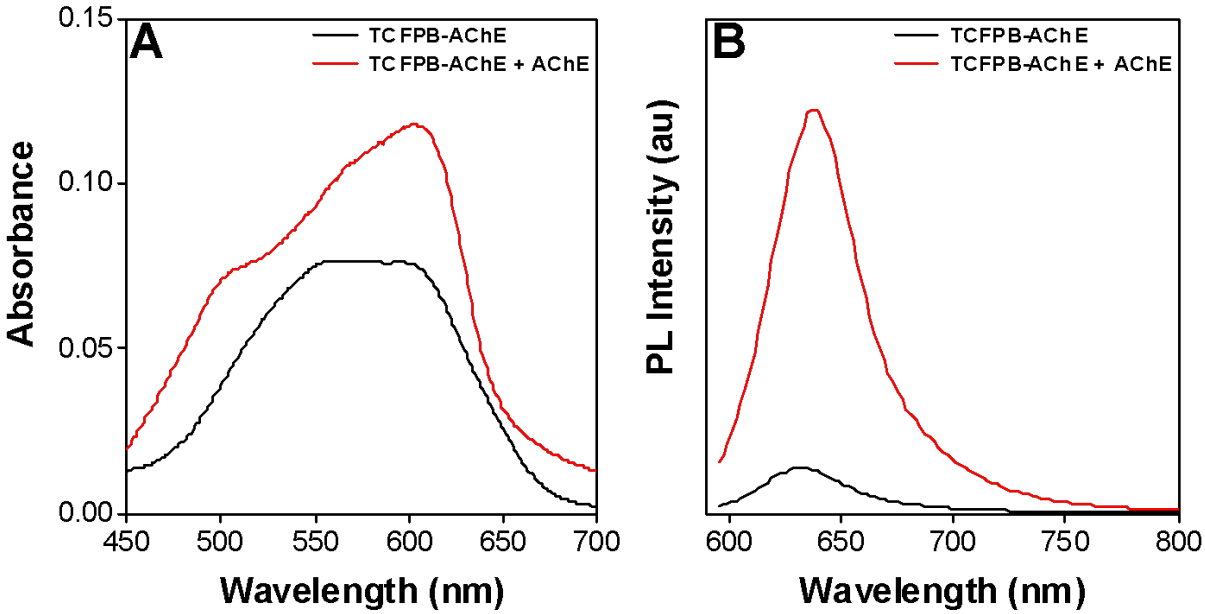

Figure S1. (A) Absorption and (B) fluorescence spectra of probe TCFPB-AChE (5 μM) in the absence (black) and presence (red) of AChE (0.2 U/mL).

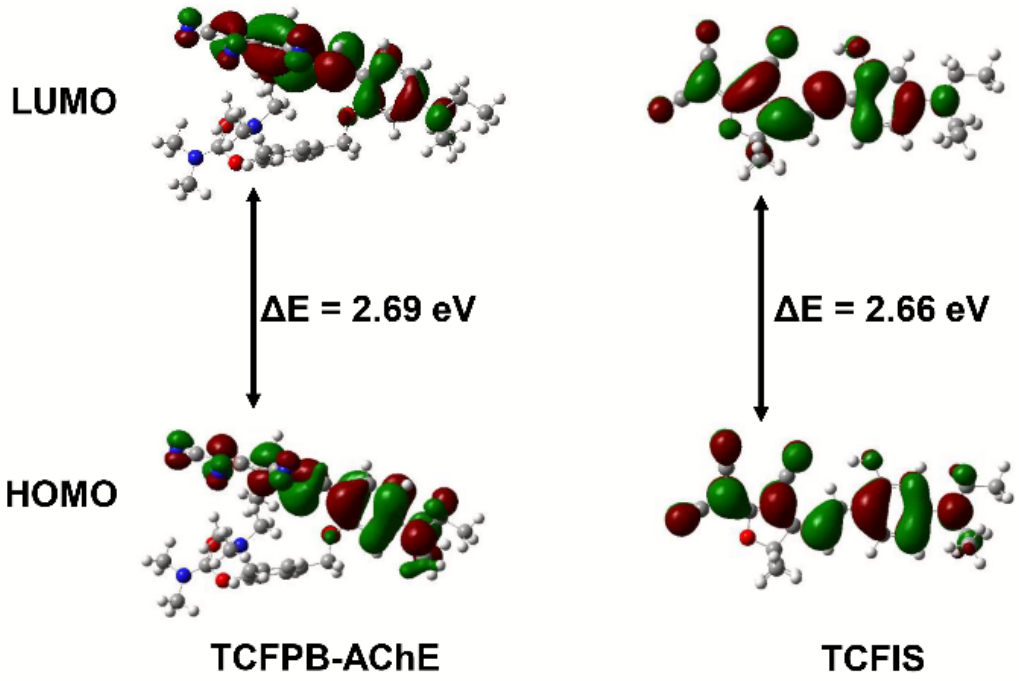

Figure S2. HOMO and LUMO of TCFIS and TCFPB-AChE were calculated by DFT method.

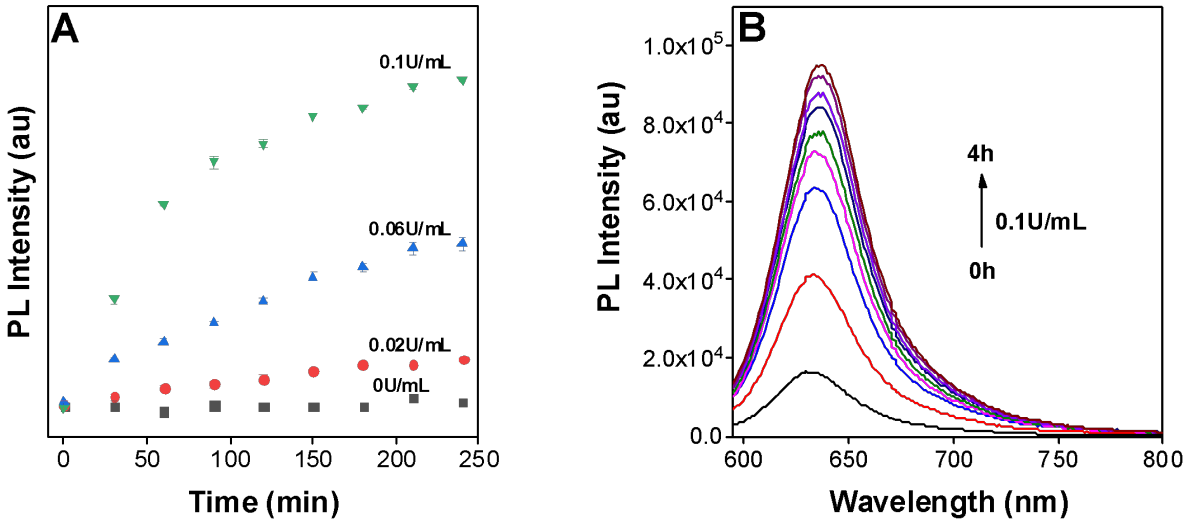

Figure S3. (A)Time-dependent fluorescence intensity (634nm) of TCFPB-AChE (5 μM) with different concentrations (0, 0.02, 0.06 and 0.1 U/mL) of AChE. (B) Fluorescence spectrum of the mixed solution of TCFPB-AChE (5 μM) and AChE (0.1U/mL) from 0 to 4 h. λ_{ex} = 575 nm.

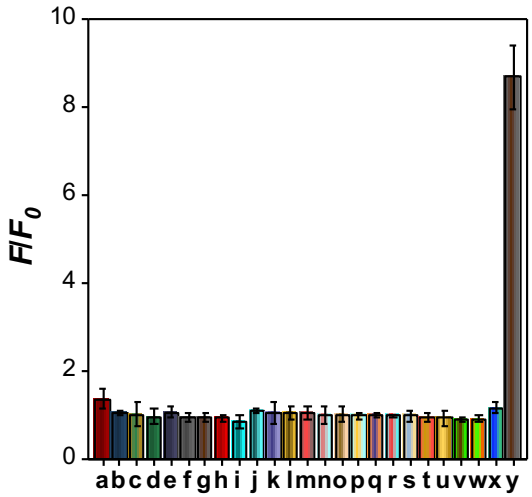

Figure S4. Variations of PL intensity (634nm) of **TCFPB-AChE** (5 μM) after incubation with 0.2 U/mL AChE and other biologically-relevant species; a: BChE (10 U/mL); b: CE (10 U/mL); c: lipase (10 U/mL); d: lysozyme (10 U/mL); e: Pepsin (10 U/mL); f: GSH (1000 μM); g: Trypsin (100 ug/mL); h: Tyrosinase(10 U/mL); i: Hcy(100 μM); j: ATP(1000 μM); k: Cys (100 μM); l: K^+ (100 μM); m: Br^- (100 μM); n: Cl^- (100 μM); o: ClO^- (100 μM); p: I^- (100 μM); q: H_2O_2 (100 μM); r: H_2S (100 μM); s: Na^+ (100 μM); t: Ca^{2+} (100 μM); u: Fe^{3+} (100 μM); v: Mg^{2+} (100 μM) w: Na_2S_4 (100 μM); x: Lactoferrin (10 U/mL). (F is the fluorescence intensity of TCFPB-AChE at 634 nm, and F_0 is the fluorescence intensity of TCFPB-AChE and analyte at 634 nm after incubation for 4 hours) y: AChE; λ_{ex} =575 nm.

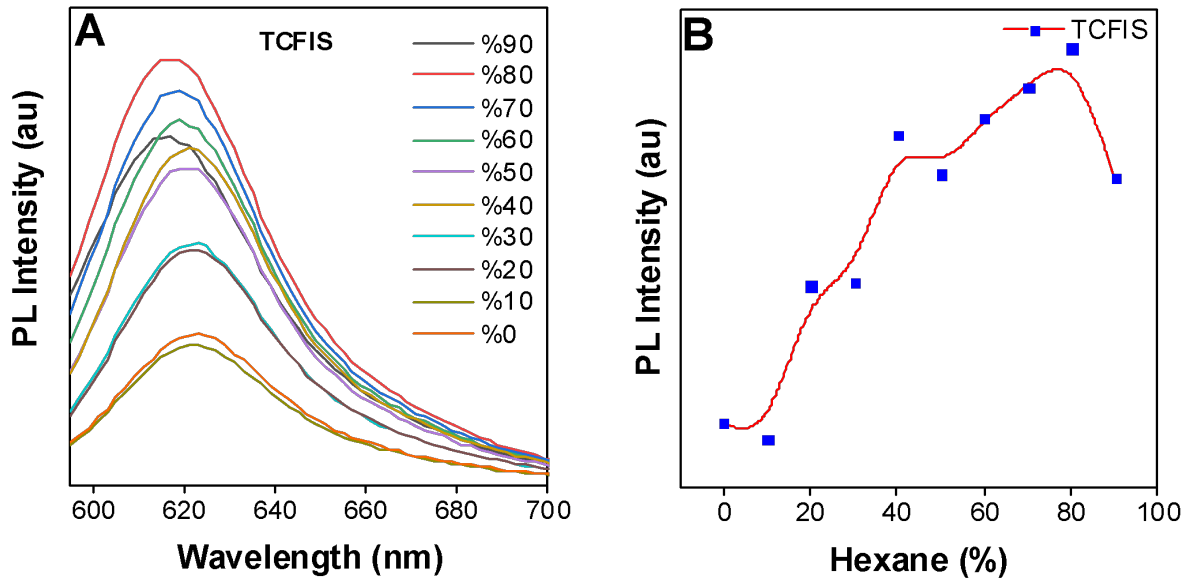

Figure S5. (A) PL spectra of **TCFIS** in ethanol/hexane mixtures with different hexane fractions. (B) The plot of PL intensity vs the composition of the ethanol/hexane mixtures of **TCFIS.** λ_{ex} = 575 nm.

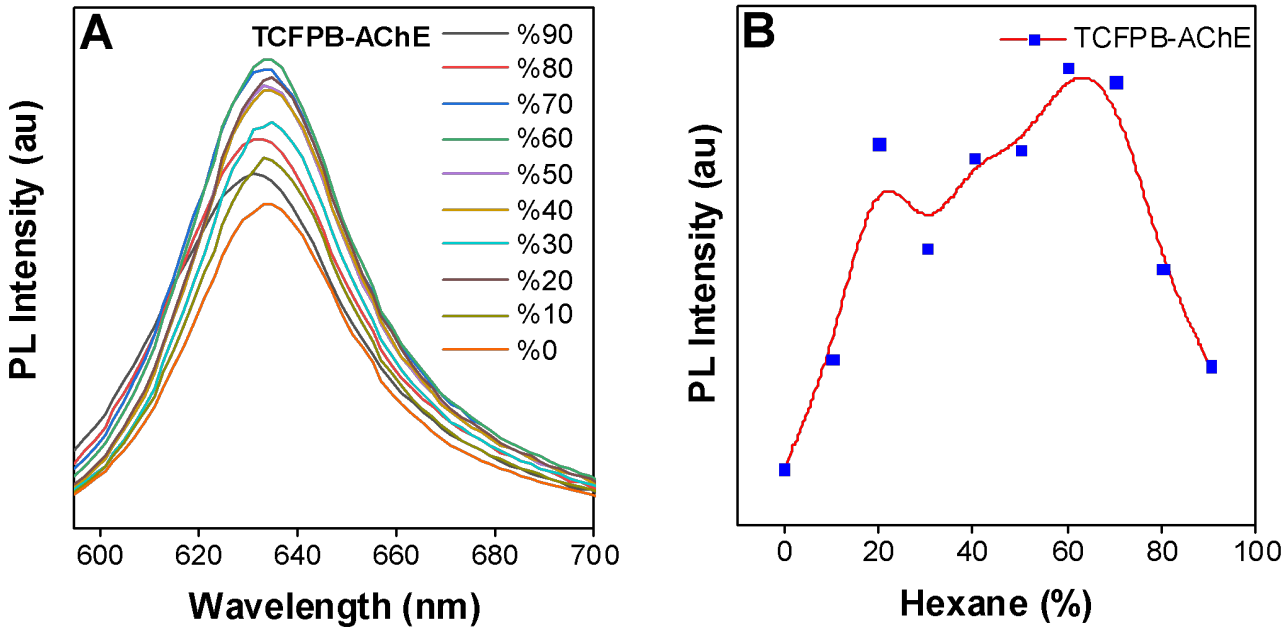

Figure S6. (A) PL spectra of **TCFPB-AChE** in ethanol/hexane mixtures with different hexane fractions. (B) The plot of PL intensity vs the composition of the ethanol/hexane mixtures of **TCFPB-AChE**. λ_{ex} = 575 nm.

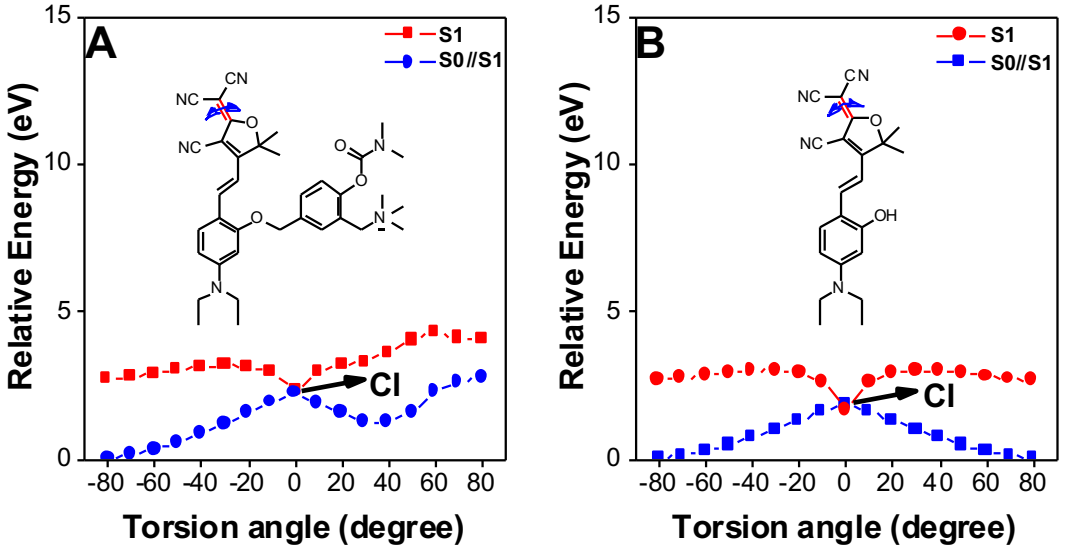

Figure S7. The potential energy surfaces of **TCFPB-AChE** (A)and **TCFIS** (B) geometries in the excited state (S_1) as a function of the torsional angles. S_0//S_1 is the ground state (S_0) projected vertically by S_1.

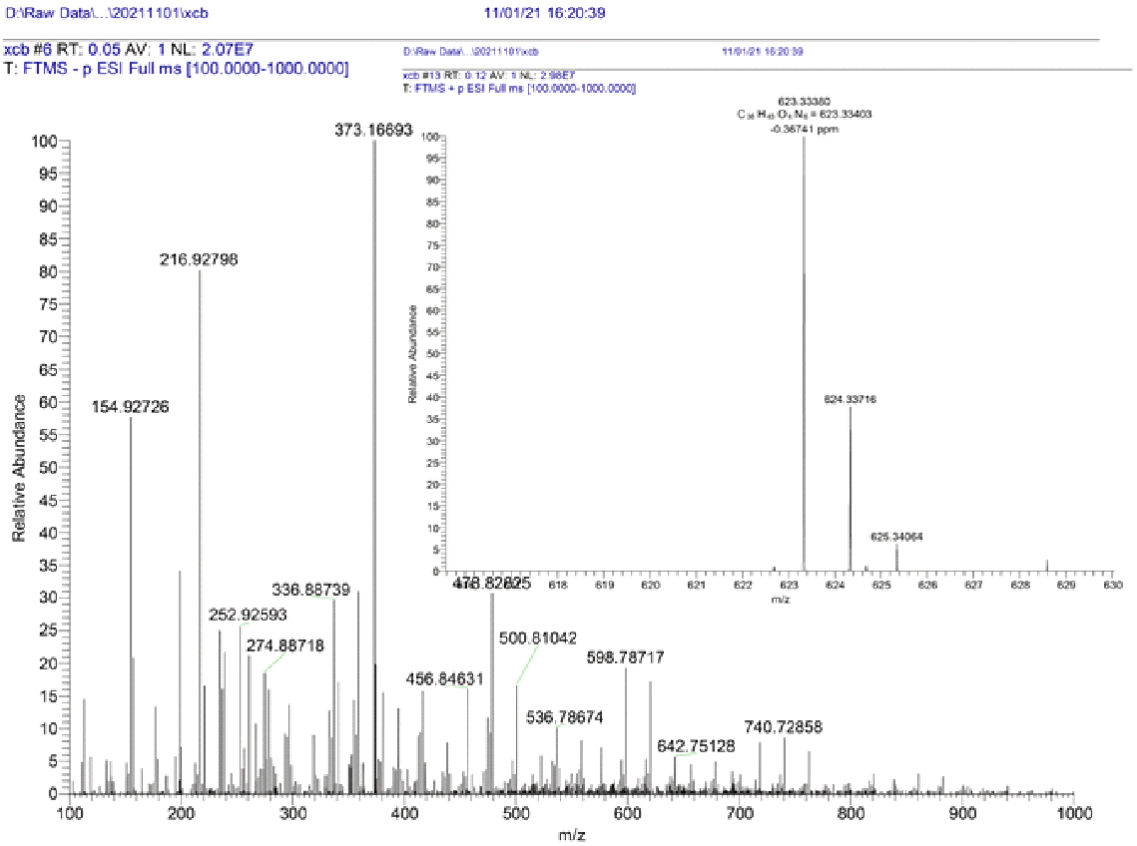

Figure S8. HRMS spectrum of **TCFPB-AChE** after incubation with AChE (0.2 U/ml) at 37 °C for 4 h. **TCFIS**([M-H]$^-$ calcd for $C_{22}H_{21}N_4O_2$: 373.16700, found: 373.16693). **TCFPB-AChE**(calcd for $C_{26}H_{26}N_4O_6$: 623.33403, found: 623.33380).

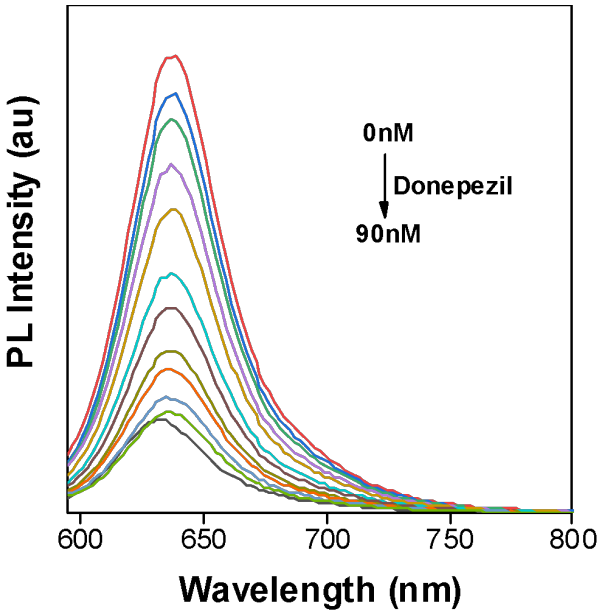

Figure S9. Fluorescence spectra of probe TCFPB-AChE with 0.2 U/mL AChE pretreated with different concentrations of donepezil ranging from 0 to 90 nM in PBS buffer (pH 7.4).

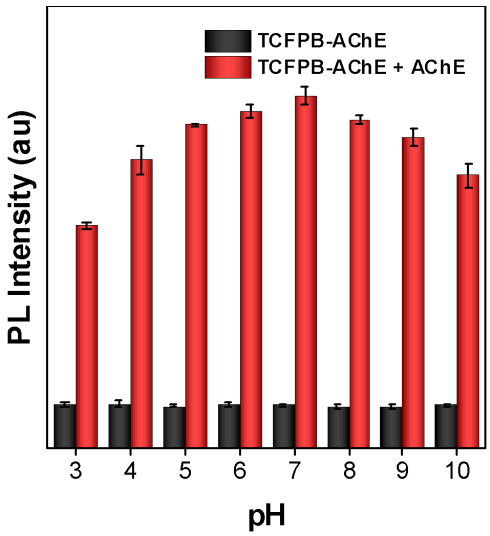

Figure S10. The PL intensity (634 nm) ratios of **TCFPB-AChE** (5 μM, black bars) and **TCFPB-AChE** (5 μM) + AChE (0.2 U/mL, red bars) in different pH buffers. λ_{ex} = 575 nm.

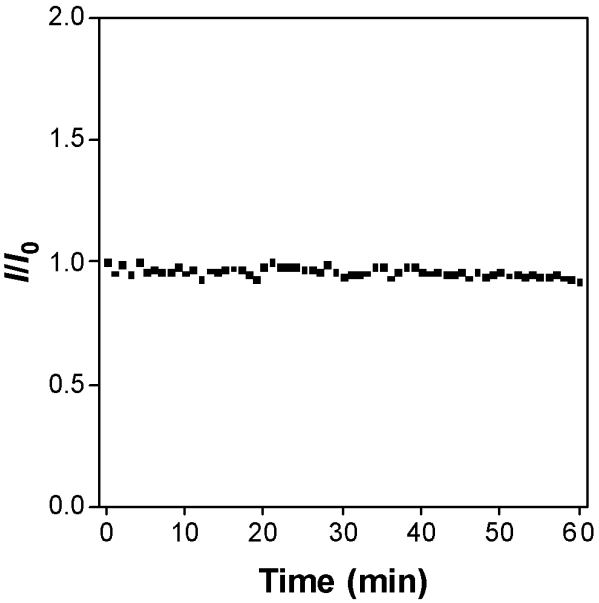

Figure S11. The light stability test of **TCFPB-AChE** in 60 min, **TCFPB-AChE** = 5 μM. λ_{ex} = 575 nm.

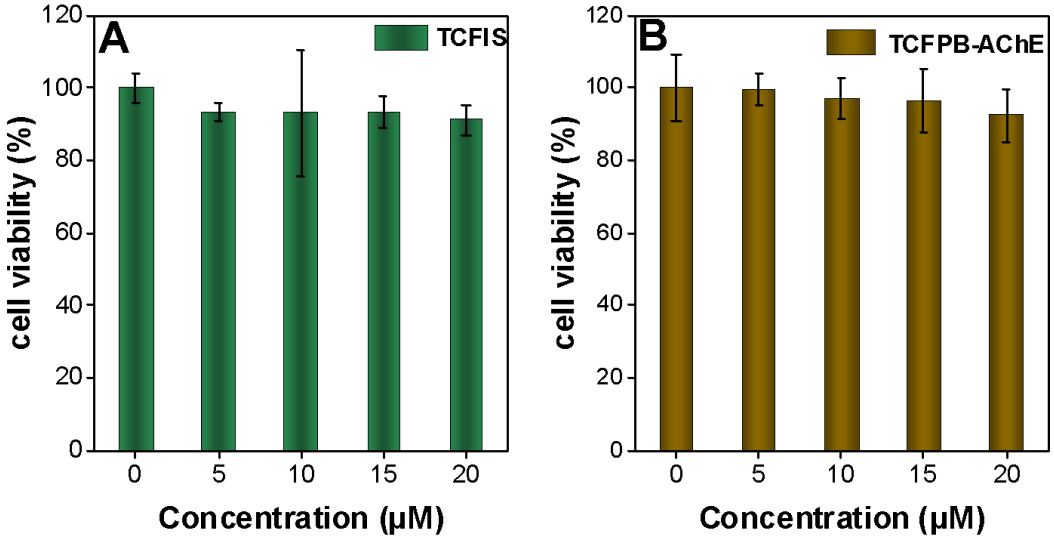

Figure S12. Cell viability of U87 cells at varied concentrations of **TCFIS** (A) and **TCFPB-AChE** (B) by using CCK8 method.

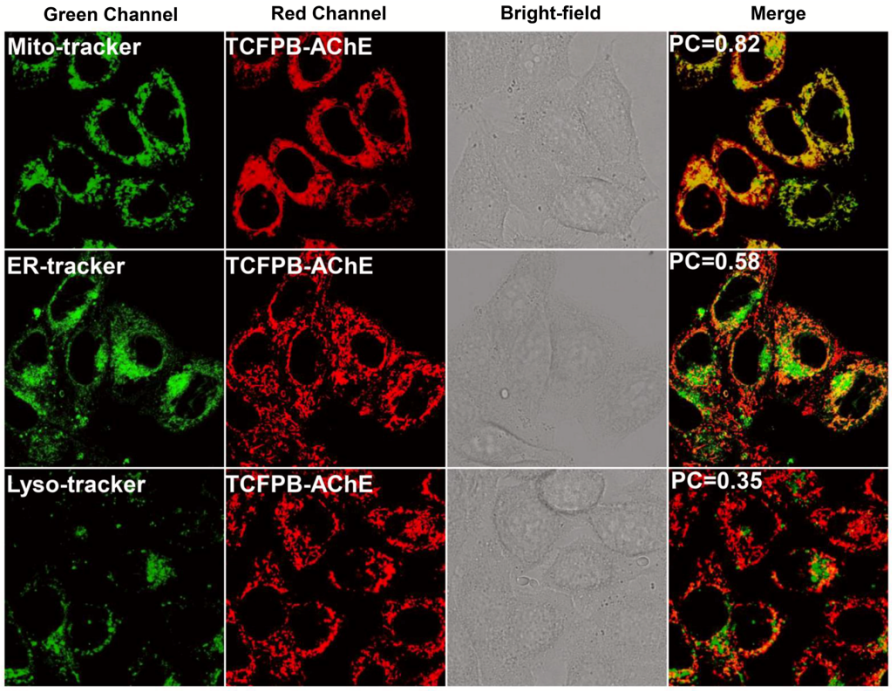

Figure S13. Colocalization experiment of TCFPB-AChE (5 μM) and various organelle trackers (100 nM) in HeLa cells, scale bar= 20 μm. TCFPB-AChE (λ_{ex}= 561 nm, λ_{em}= 600-700 nm). Subcellular organelle tracker (λ_{ex}= 488 nm, λ_{em}= 500-550 nm).

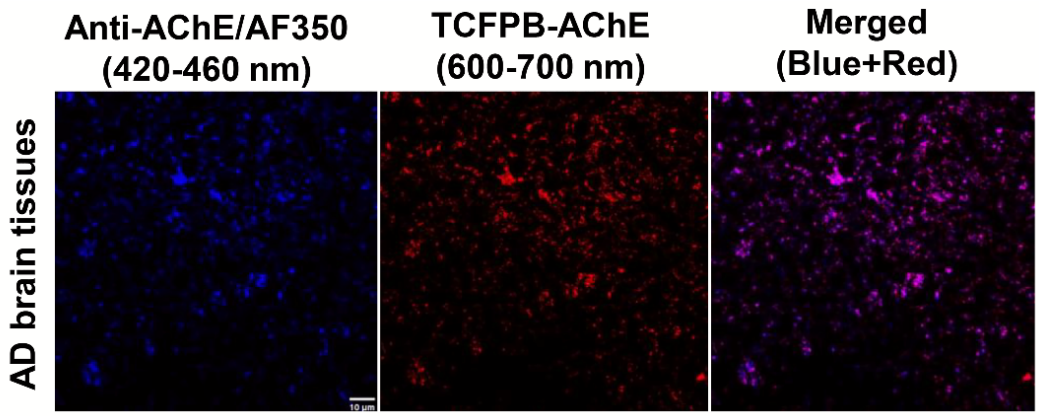

Figure S14. Fluorescent staining of AChE with TCFPB-AChE(1 μM, λ_{ex}= 561 nm) and Anti-AChE/AF350 (10 μg/mL), λ_{ex} = 405 nm) in AD brain tissues. Scale bar= 10 μm.

Table S2. Comparison of reported fluorescent probes for AChE detection.

References	Response mode	Detection limit	$\lambda_{ex}/\lambda_{em}$ (nm)	Biological application
Angew. Chem. 2007, 119, 8028 –8032	ACQ	0.05 U/mL	376/424	/
J. Am. Chem. Soc. 2019, 141, 2061−2068	ACQ	0.36 U/mL	520/560	Cells and in vivo imaging

Anal. Chem. 2020, 92, 13405−13410	ACQ	0.127 U/mL	545/654	Cells, zebrafish and tissues imaging
Journal of Hazardous Materials .2021,410 ,124811	ACQ	0.2 U/mL	365/450	Cell imaging and mouse blood analysis
ACS Sens. 2020, 5, 83−92	ACQ	0.1173 U/mL	670/700	Cells and zebrafish imaging
Chem. Sci., 2020, 11, 11285–11292	ACQ	0.017 U/mL	550/582	Cells, tissues and in vivo imaging
J. Mater. Chem. B, 2021, 9, 2623–2630	ACQ	0.21 U/mL	680/740	Cells, tissues and in vivo imaging
This work	AIE	0.009355 U/mL	575/634	Cells, tissues and in vivo imaging

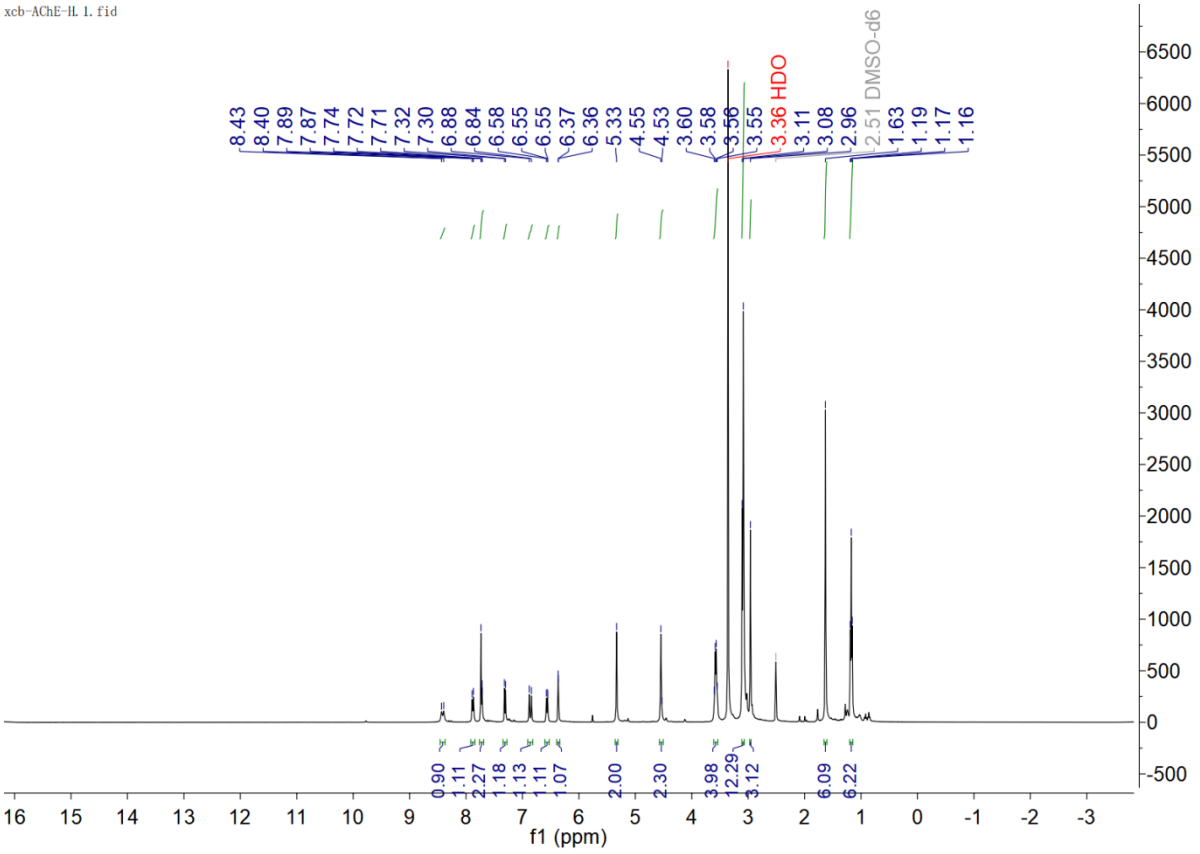

Figure S15. ^{1}H NMR spectrum of **TCFPB-AChE** in d_6-DMSO.

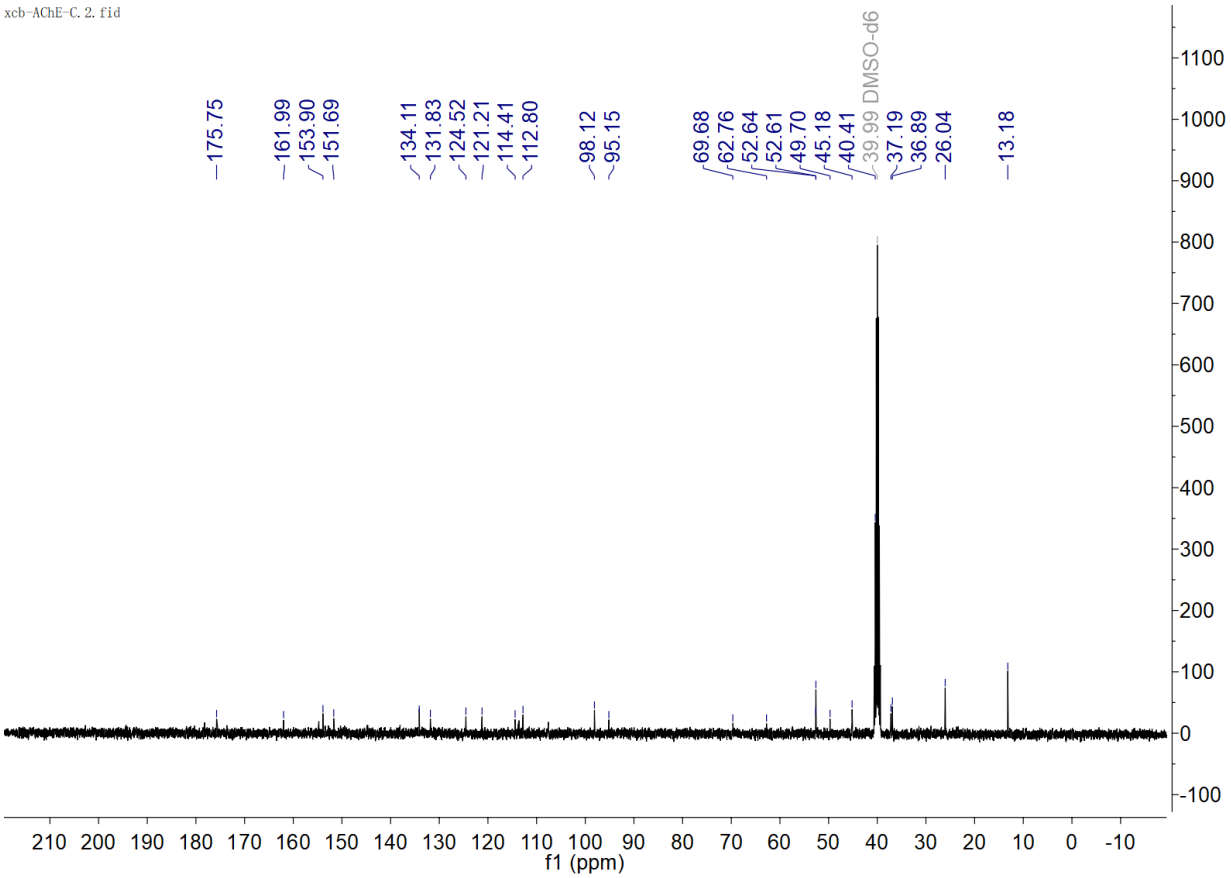

Figure S16. ^{13}C NMR spectrum of **TCFPB-AChE** in d_6-DMSO.

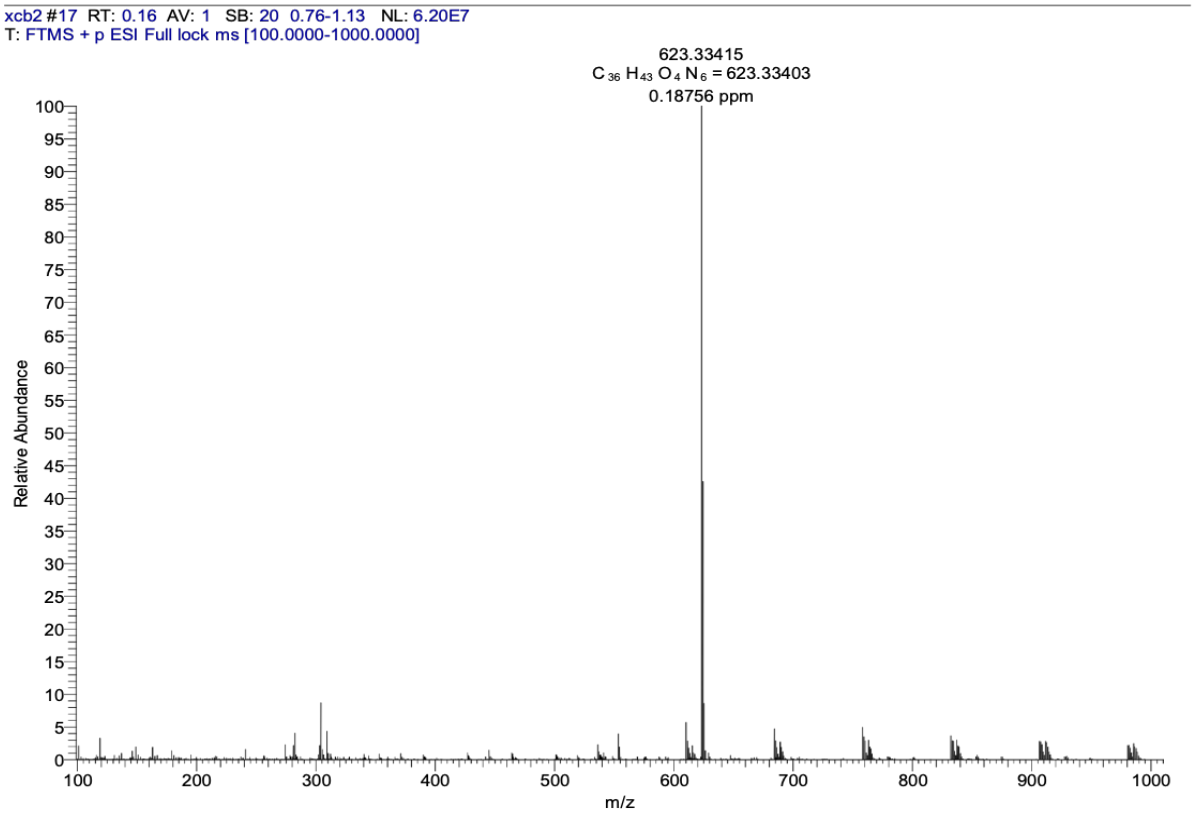

Figure S17. HRMS spectrum of **TCFPB-AChE**.

References

1. C. Xiang, C. Li, J. Xiang, Y. Luo, J. Peng, G. Deng, J. Wang, S. Kolemen, H. Li and P. Zhang, An easily available lysosomal-targeted ratiometric fluorescent probe with aggregation induced emission characteristics for hydrogen polysulfide visualization in acute ulcerative colitis, *Mater. Chem. Front.*, 2021, **5**, 7638-7644.
2. X. Wu, J. M. An, J. Shang, E. Huh, S. Qi, E. Lee, H. Li, G. Kim, H. Ma, M. S. Oh, D. Kim and J. Yoon, A molecular approach to rationally constructing specific fluorogenic substrates for the detection of acetylcholinesterase activity in live cells, mice brains and tissues, *Chem. Sci.*, 2020, **11**, 11285-11292.
3. M. Rajeswari, N. Santhi and V. Bhuvaneswari, Pharmacophore and virtual screening of JAK3 inhibitors, *Bioinformation*, 2014, **10**, 157.
4. R. Fazi, C. Tintori, A. Brai, L. Botta, M. Selvaraj, A. Garbelli, G. Maga and M. Botta, Homology model-based virtual screening for the identification of human helicase DDX3 inhibitors, *J. Chem. Inf. Model.*, 2015, **55,** 2443-2454.